On site characterization and air content evaluation of coastal soils by image analysis to estimate liquefaction risk

Article *in* Canadian Geotechnical Journal · December 2008

DOI: 10.1139/T08-090

CITATIONS
4

READS
8

3 authors, including:

Pierre Breul
Université Blaise Pascal - Clermont-Ferrand II
61 PUBLICATIONS **140** CITATIONS

SEE PROFILE

On site characterization and air content evaluation of coastal soils by image analysis to estimate liquefaction risk

P. Breul, Y. Haddani, and R. Gourvès

Abstract: Coastal structures are often submitted to intense wave forcing. In some cases, structures may have stability disorders due to the constant weakening of their foundations and to momentary liquefaction of the sea bed. Studies have shown that if classical geotechnical characterization is a necessity, air content in the soil is also a key parameter for liquefaction evaluation. That is why on site air content measurement and its time variation during a tide period may provide information and help to determine a better understanding of this problem. Unfortunately, this parameter is difficult to measure during investigations. This article presents a technique based on the use of geoendoscopy and automatic image analysis, which makes it possible to characterize coastal soils and to estimate their air content. After a description of the technique, the results obtained on laboratory tests and on a real site are presented.

Key words: geoendoscopy, image analysis, liquefaction, air content, on site soil characterization.

Résumé : Les structures côtières sont soumises à la sollicitation de la houle. Ces sollicitations cycliques peuvent être intenses et entraîner parfois des instabilités dues à des pertes de portance du sol sur lequel reposent les structures par la création de phénomènes de liquéfaction locaux. Des études ont montré que l'apparition de ces phénomènes était fonction notamment de la teneur en air occlus dans le sol. C'est pourquoi, la mesure de la teneur en air in situ et de son évolution durant un épisode de marée peut permettre de comprendre ou d'apporter des pistes de réflexion pour résoudre le problème. Or cette caractéristique est à l'heure actuelle difficilement mesurable in situ ou en laboratoire et difficilement maîtrisable lors de la réalisation d'expérimentation. C'est pourquoi la recherche de techniques permettant de mesurer ou d'estimer la teneur en air occlus d'un sable est importante. La technique proposée ici s'appuie sur l'utilisation de la géoendoscopie et de l'analyse d'images. En effet, les essais réalisés avec cette technique ont montré qu'il est possible d'identifier très clairement la présence d'air au sein du matériau et de venir effectuer une mesure à partir des images acquises. Cette communication présente le contexte de l'étude, la technique utilisée puis les essais réalisés aussi bien in situ en conditions réelles qu'en laboratoire et les résultats obtenus.

Mots-clés : géoendoscopie, analyse d'images, liquéfaction, teneur en air, caractérisation des sols in situ.

Introduction

Coastal structures often experience wave forcing. In some cases, these cyclic stresses may be intense and involve instabilities by the creation of the local phenomenon of liquefaction. Theoretical models have highlighted this phenomenon (Mei and Foda 1981; Sakai et al. 1992).

According to many authors (Seed 1986; Rad and Lunne 1994; Rad et al. 1994; Robertson and Wride 1998; Grozic et al. 1999, 2000), the apparition of the liquefaction phenomenon is conditioned by the characteristics of the stress and also by the nature and the state of the soil. A parameter called the potential of liquefaction has been defined that expresses the ability of a ground to reach this state. It is based on the knowledge of the cyclic stress ratio for a reference magnitude of 7.5 on the Richter scale ($CSR_{7.5}$) (Seed 1986) and the cyclic resistance ratio for a reference magnitude of 7.5 ($CRR_{7.5}$). This last parameter is usually obtained from in situ tests (e.g., standard SPT or CPT) and from geotechnical soil properties such as fine particles content and particle size distribution (Seed 1986; Robertson and Wride 1998). In the case of soils submitted to breaking waves, previous parametric studies of the models have shown that the occurrence of momentary liquefaction would also be highly sensitive to air content inside the soil (Rad and Lunne 1994; Rad et al. 1994; Gratiot and Mory 2000; Grozic et al. 2005).

It is difficult to obtain these characteristics on site with classical geotechnical tools. Moreover, the development of representative laboratory tests concerning air content is still delicate. This is why we have worked on developing new tools to characterize these features on site. The new technique proposed in this article is based on the use of geoendoscopy (Breul 1999).

This article begins with a description of the general methodology based on the use of geoendoscopy. The experimental site and the geotechnical soil properties obtained by using this device are described next, and lastly, theair content assessment within the coastal soil is reported on.

Received 20 September 2006. Accepted 22 August 2008. Published on the NRC Research Press Web site at cgj.nrc.ca on .

P. Breul[1] and R. Gourvès. LGC – C/U/S/T Université Blaise Pascal – Clermont II. Campus Cézeaux. 24, av. des landais, BP 206, 63,174 Aubière CEDEX France.
Y. Haddani. Sol Solution ZA des portes de Riom 63200 Riom.

[1]Corresponding author (e-mail: breul@lgc.univ-bpclermont.fr).

Fig. 1. General methodology of characterization.

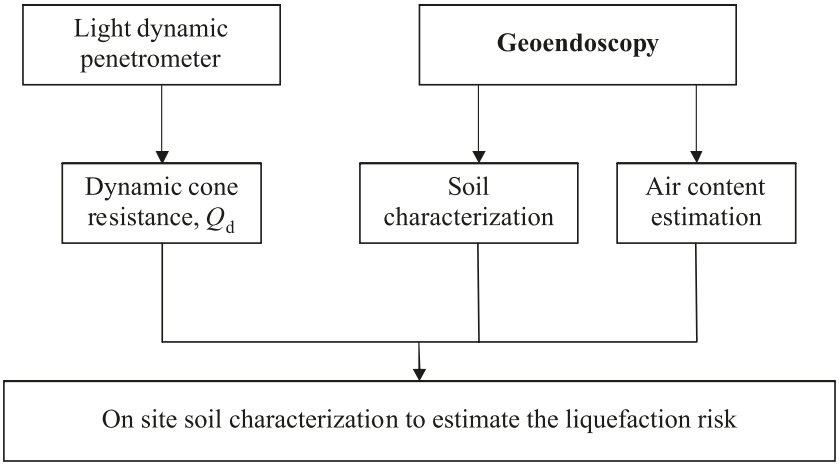

Fig. 2. Scheme and picture of the endoscopic device.

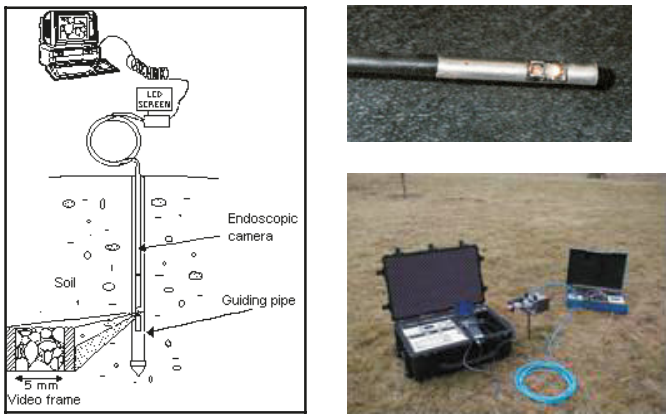

Methodology and geoendoscopy

Proposed methodology

As previously mentioned, the occurrence of liquefaction phenomena in coastal soils is conditioned by three factors: the physical soil properties, the density, and the air content. The evaluation technique of the liquefaction risk must then characterize these three features. Moreover, the proposed methodology must be adapted to the particular context of the coastal area (saturated and underwater soil, difficult access, delicate recording measurement conditions). The methods of Seed (1986) and Robertson and Wride (1998) are the most used among the in situ methods of liquefaction potential determination quoted by Glaser and Chung (1998).

The success of these methods rests firstly on the use of familiar and widespread geotechnical tests (SPT and CPT), and secondly on the existence of a wide data bank. However, these methods have some drawbacks.

Seed's method (Seed 1986) relies on the use of the SPT, which can reach its limits in terms of reliability in weak resistance soils in particular (Lepetit 2002). Moreover, this method requires laboratory tests to characterize soil.

In the Robertson method (Robertson and Wride 1998), the soil characterization is done on site by the measurement of the sleeve friction, which is related to grain size distribution. This method is not cost effective because the implementation of the CPT test remains difficult and expensive in coastal areas.

The methodology suggested here relies on the use of light tools developed within LGC (Fig. 1). The Panda (Gourvès 1991), which is a light penetrometer, provides the dynamic cone resistance of the ground according to the depth. The geoendoscopy (Breul 1999) records soil images from which a physical and morphological characterization of the soil is realized thanks to image processing. Several studies (Zhou 1997; Chaigneau 2001; Lepetit 2002; Lepetit et al. 2002; Bacconnet et al. 2005) have shown the interest and the reliability of the measurements carried out with the Panda. The tests and results obtained with this device on this experimentation are not presented here; they can be found in the paper by Bonjean et al. (2004).

Geoendoscopy

Geoendoscopy (Fig. 2) has been developed by the LGC and used for several years (Breul 1999; Haddani 2004) to provide in situ soil geotechnical characterization either on sites where the sampling is constraining or difficult to access or to reduce long and expensive laboratory tests (particularly for undisturbed samples).

This technique uses a video-endoscope (8.6 mm diameter). Videocolour images 25 mm^2 in area (640 $\times$ 480 pixels) with a ten-fold magnification are acquired from a cavity in the soil. Signal treatment or image analysis processing enables the determination of the different soil parameters (particle size and shape analysis, texture, stratigraphy, contact orientations etc.). The video endoscope technique is usually associated with classical geotechnical tests, such as penetration tests. Information obtained from image analysis can be coupled with the mechanical parameters measured at the same location.

This technique has been widely used for unsaturated soils, but is rarely used for underwater soils. Other researchers (Köhler and Koenders 2003) have used this technique to obtain a direct visualization of underwater phenomena in soil–fluid interactions. However, these tests were only carried out in the laboratory and remain primarily qualitative.

Fig. 3. (*a*) Set-up for the video-endoscope on the bunker wall. (*b*) Instrumented bunker wall facing the ocean. (*c*) Test investigation during tidal conditions. (*d*) General view of the experimental site.

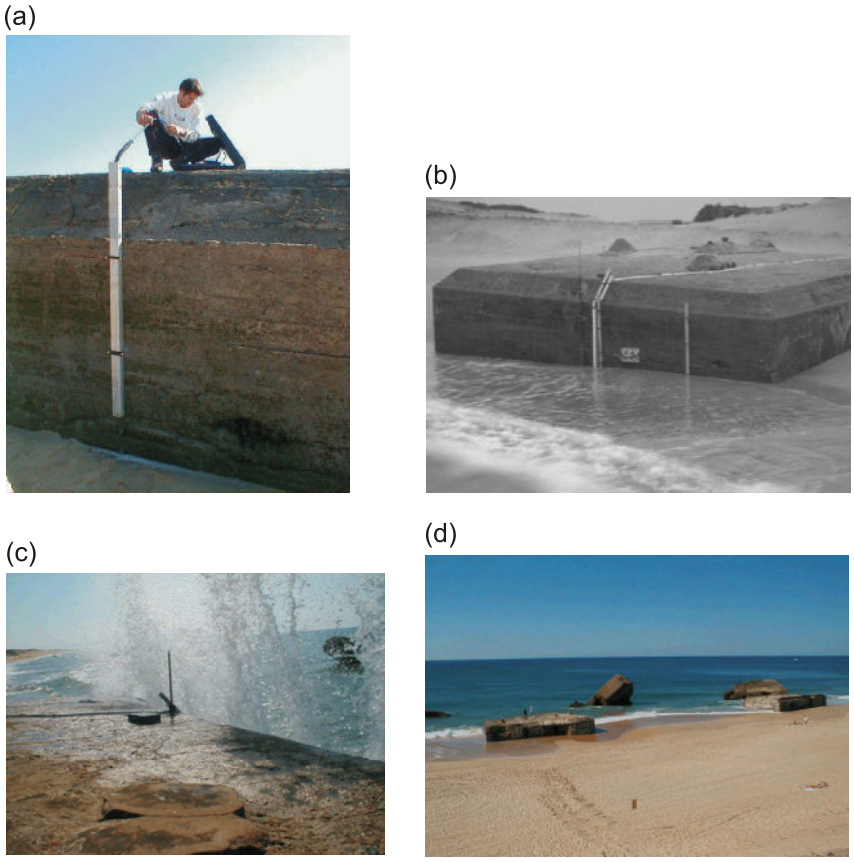

Fig. 4. Examples of images recorded with the geoendoscope during tide.

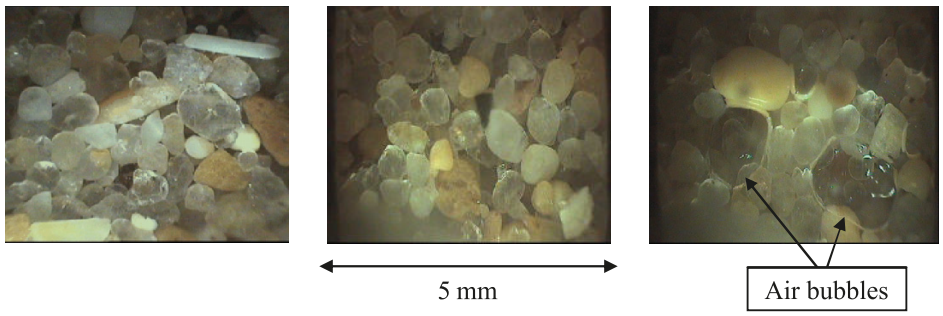

Experimental site description and on site geotechnical soil characterization

Experimental site description

The field experiment was carried out at Capbreton, 30 km north of Biarritz on the Atlantic coast of Aquitaine, in the southwest of France. The site was selected on the one hand because the sandy coast of Aquitaine is subject to strong wave activity (Howa et al. 1999), and, on the other hand because of the possibility of instrumenting real structures (bunkers from the Second World War in fact) directly exposed to the wave action (Fig. 3). Field experiments were carried out during periods of high tide conditions, that is, when the bunkers were partially submerged at full tide (with a mean water depth of about 2 m) and fully emerged at low tide.

The bunker was instrumented at two locations (Fig. 3) (in the middle of the wall facing the ocean and at the corner) with different systems: pore pressure sensors at different depths inside the bed, bed level monitoring, flow velocities, and wave height measurements in the vicinity of the bunker.

For the geoendoscope, a 14 mm diameter Plexiglas tube equipped with a conical tip was pushed into the soil and then fixed onto the bunker (Fig. 3). The tube was watertight enabling the video-endoscope to be freely displaced inside the tube to monitor the soil at different depths.

To avoid the eventual impact on the air content measurement (see section entitled "Laboratory air content measurements") caused by the introduction of the tube , the tube was placed at residence on the bunker (Fig. 3). Once the instrumental setup was complete, we waited until a complete

Fig. 5. Evolution of the sand bed during the tide compared to the initial position.

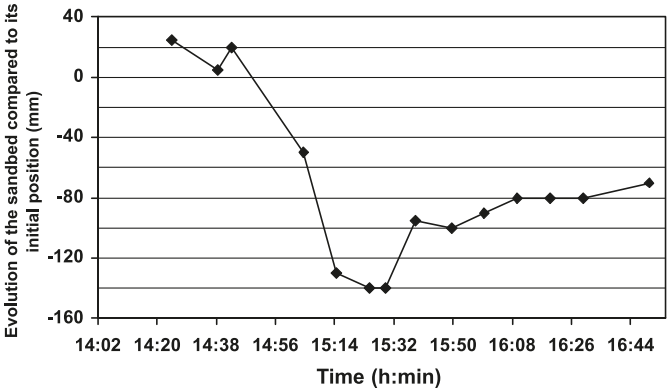

tide passed before making measurements during subsequent tides (on a ground considered to be undisturbed).

Eight tests were carried out around the bunker at different moments during a tide period. The tests were carried out at depths down to 1.10 m from the sea bed.

One test was carried out during a complete tide period with a regular frame grabbing ranging from 5 min to half an hour (according to the evolution of the tide). Sediment particles and air bubbles can easily be distinguished on the soil images. Some examples are shown in Fig. 4.

On site soil characterization

Sand bed variations

Endoscopic investigations yielded very interesting information during the high tide period about the sand bed underneath the wall facing the ocean. It is possible to observe the limit between the sand bed and the water when no wave is breaking and the water is carrying low suspension. The evolution of this limit during a tide is shown in Fig. 5.

In addition, we were able to observe the displacements of sand particles within a mobile layer as well as the thickness of this mobile layer. Thus, with this equipment we can determine the following for any given wave: the part of the sand bed that is subjected to visible strains, the part of the sand that is not disturbed by the wave action, and the depth of the frontier between these two areas. Qualitative analyses made it possible to determine that only some few centimetres (about 3–5 cm) of sand were moved during the passage of a wave.

Geotechnical soil properties

Once the images were acquired, our work consisted of extracting relevant geotechnical information and developing automatic analyses to derive reliable values of the studied characteristics.

To achieve this goal, we set up the following image analysis procedures of characterization (Breul 1999; Haddani 2004):

- Texture determination of the granular media allowing for the characterization of relative smoothness or roughness and for the assessment of its fine particles content,
- Particle size analysis. The grading curve can be calculated by image analysis for materials having grains lower than 5 mm and a fine elements percentage lower than 12%,
- Colorimetry: these features are used for the automatic stratigraphy of a soil.

In this case, we carried out texture analysis, which is based on a spectral and statistical analysis computed on treated grey level images. Figure 6 shows the results obtained for each one of these parameters and for two tests located, respectively, in front of and behind the bunker. The analysis of the performed tests shows a good homogeneity of sand features with the depth and a relatively low space variability. These results confirm the visual analyses carried out on the spot at the time of the tests. The sand grain size distribution did not appear to vary significantly with time. The intermittent deposition of limited quantities of gravel of a few millimetres on the sandy bed was only noticed on a few occasions.

Automatic particle size analysis (Breul 1999; Breul et al. 1999) from the acquired images was carried out to make comparisons with collected samples in the vicinity of the bunker. The comparison of the results obtained with the traditional grain size distribution by sieving and the results obtained by image analysis are provided in Fig. 7.

The results obtained with both methods show a good agreement and provide a similar grain size distribution ranging from 0.2 to 1.5 mm.

The on site geoendoscopic analysis highlighted the fact that sand surrounding the site of the experiment had relatively homogeneous characteristics and hence one could characterize its particle size distribution.

To determine all of the information on the soil characterization according to the liquefaction potential, the air content must be assessed.

Air content evaluation inside the soil

The characterization and the identification of soils likely to liquefy is not sufficient to estimate the potential of liquefaction. Indeed, for soils exposed to the swell, the air content within the saturated soils is also important. Unfortunately the measurement of this parameter remains touchy in the laboratory and it is not technically possible to realize on site at the present time. A soil sampler for measuring gas content was designed in the course of the European project LIMAS, but for operational reasons it could not be tested during the final trial. The device has been tested during separate experiments, and it is actually still in development (Sandven et al. 2007). This is why the idea to use the geoendoscopy to estimate the air content on site was tested. Before carrying out tests in real conditions, laboratory tests were performed to study the technical feasibility of the method and to study its potential for measurement (Breul and Gourves 2003).

Tests of feasibility in the laboratory

Description of the tests

Tests were carried out within a tank (Fig. 8), which was separated into two parts. One part contained clean sand of expanded density (loose state) set up by "package"; the

Fig. 6. Comparison of the evolution of image texture parameters for tests 4 and 8.

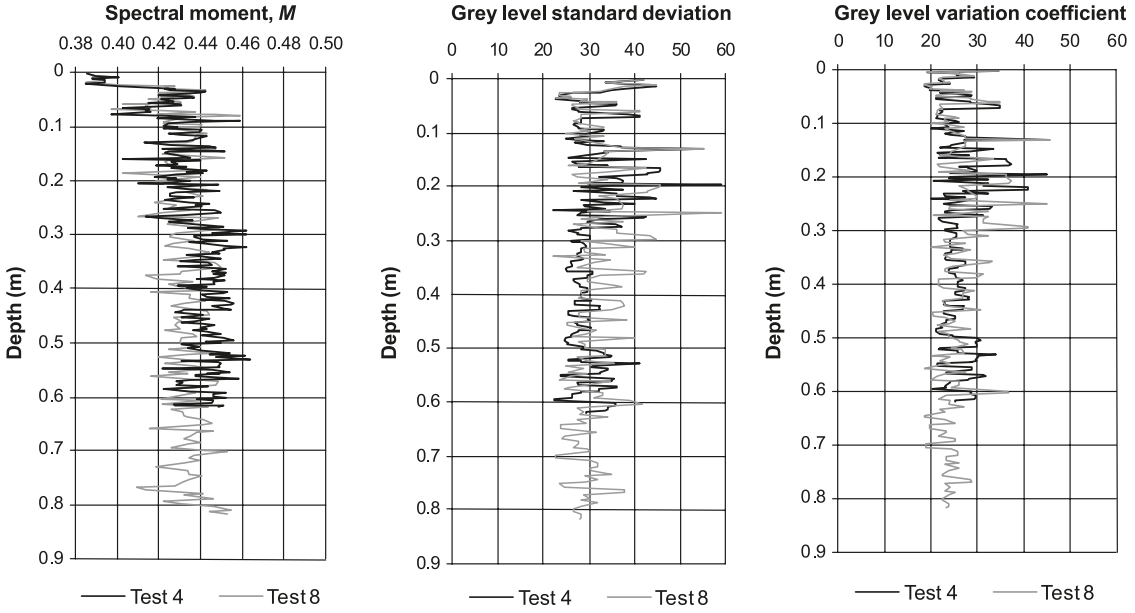

Fig. 7. Particle size analysis: sieve and image analysis comparison.

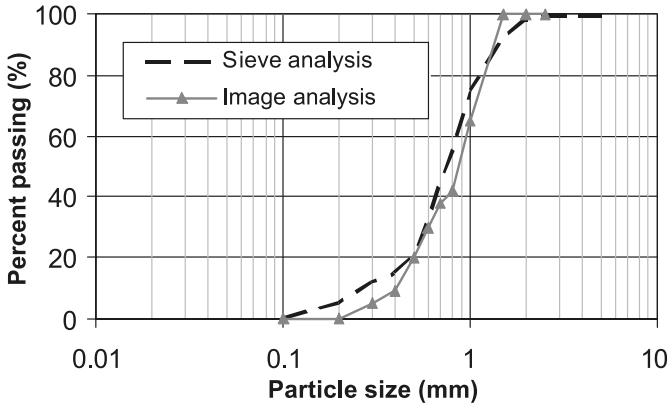

other part contained the same sand but in a denser state and set up by pluviation.

Six tests were carried out: three in each zone. Of the three tests realized in each zone, two were carried out with a glass guiding tube and one with a Plexiglas tube. Only the tests with the glass tubes were analyzed because the images obtained by this means were more exploitable. Before being able to analyze the images, it was necessary to treat them to homogenize their characteristics between each test (lighting in particular) and to extract objects of interest (in our case, bubbles of air) (Fig. 9). The treatment process is not presented in detail here. The laid down objectives were to have a robust, simple, and fast treatment, to have little time-consuming analysis of each image, and to have a fast and operational application. The treatment is based initially on the extraction of the reflection zones of the image, which are treated individually. The second step consists of transformations that improve the contrast and the dynamics of the image. Finally, a procedure was developed to extract the air bubbles from the air and to sort them according to their morphological parameters. Once the images were treated, each extracted air bubble was indexed and analyzed (surface, Ferêt diameter, circularity, centre of gravity, elongation, etc.). Only bubbles with a minimum diameter ≥50 μm can be extracted using this treatment.

Laboratory air content measurements

To summarize, the laboratory results were focused on three specific parameters:

- the number of air bubbles per analyzed image area,
- the average surface of the bubbles by image (given in pixels),
- the "surfacic air content ratio", denoted A_{Ag}, defined as the ratio of the area filled with air bubbles to the total area of the image (given in %).

The charts giving the evolution of these parameters according to depth and for each type of sand are provided in Figs. 10*a*, 10*b*, and 10*c*. The general tendencies obtained for each test are provided in Table 1. The analysis of these results shows that using the averages of the tests, it is possible to dissociate the two different density state sands. Indeed, tests 1 and 2 were carried out in the low density sand that was set up coarsely. Because of this mode of deposit, much of the air was probably trapped in the intergranular vacuums of the material, which contains macropores. Tests 3 and 4 were carried out on a relatively dense sand, which was set up by pluviation, where the air was evacuated causing the air to form finer bubbles.

In the case of the low density sand that was set up coarsely, the number of trapped air bubbles is more important and the bubbles are larger than in the dense sand that was set up by pluviation. This phenomenon ends up yielding a higher surfacic air content in the low density sand.

Tests 1 and 2 (in the expanded density sand) can be divided into two parts (Fig. 10). The first part is between 0 and 25 cm where an increase in the size of the bubbles is noticed (from 200 to 350 pixels on average) which results in an increase in the surfacic air content ratio (from 4% to more than 8%). The number of bubbles trapped remains relatively constant. Then, from 25 cm to the end of the test, a

Fig. 8. Test tank scheme.

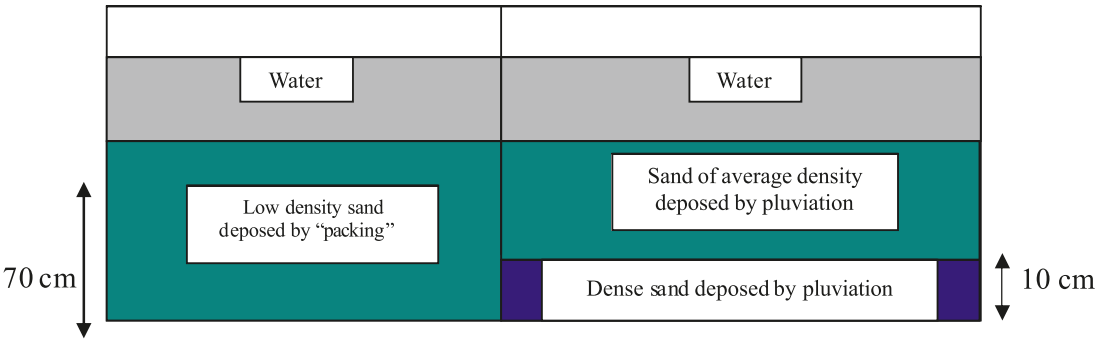

Fig. 9. Example of acquired image and extracted bubbles (after treatment).

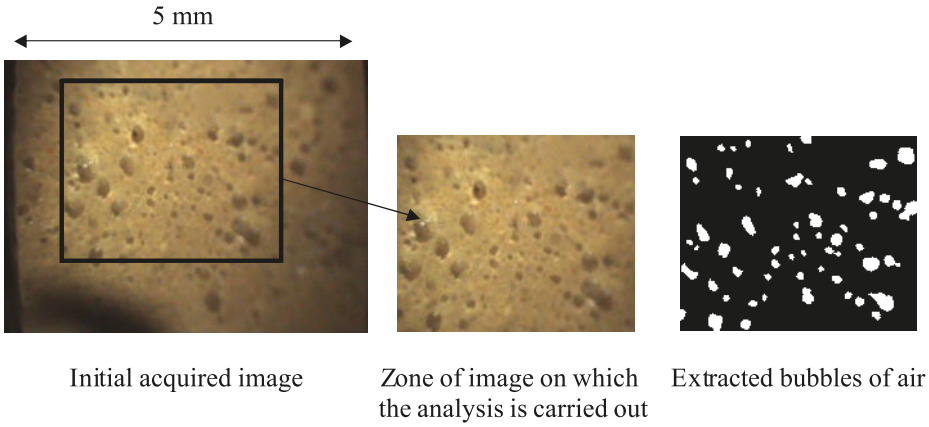

Fig. 10. For a sand with different densities: (*a*) evolution of the surface air content ratio versus depth, (*b*) evolution of the average bubble surface (pixel) versus depth, and (*c*) evolution of the number of air bubbles versus depth.

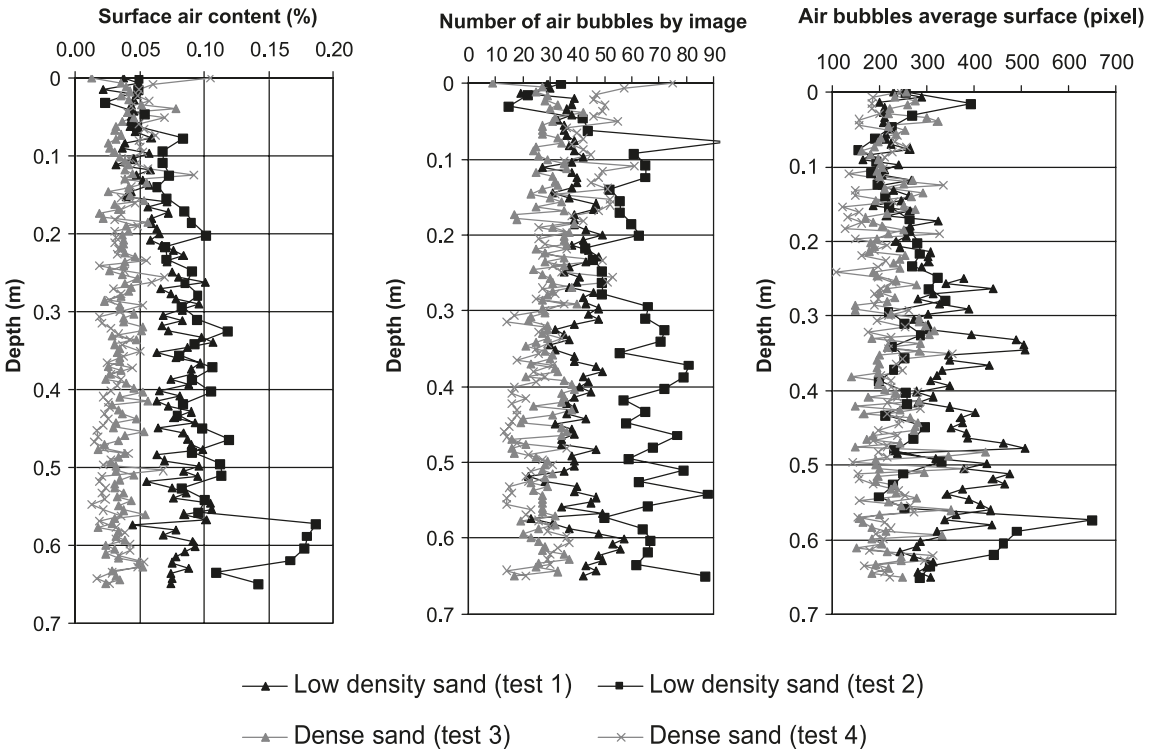

Table 1. Characteristics of the air bubbles for the various tests.

	Average number of air bubbles by image	Average surface of bubbles by image (pixel)	Average surface air content ratio (%)
Loose sand			
Test 1	39.5	314	0.07
Test 2	38.2	278	0.09
Dense sand			
Test 3	28.6	225	0.04
Test 4	32	211	0.04

Fig. 11. (*a*) Example of acquired image during the tide. (*b*) The same image after treatment to extract air bubbles.

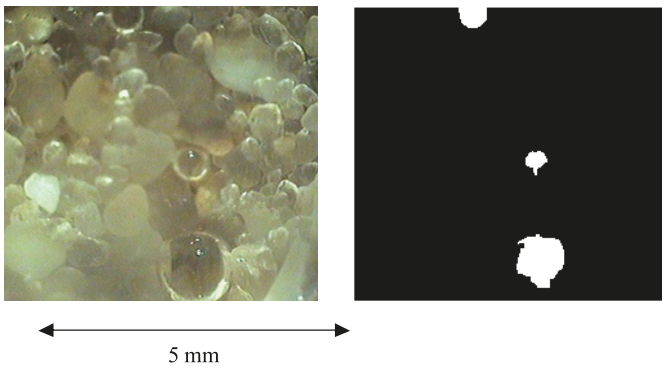

stagnation of the various parameters (around 350 pixels for the surface of the bubbles, 8% for the air content ratio, and 40 bubbles per image) is observed with important variations.

The first phenomenon (regular increase in the values of the surfacic bubble parameters) can be explained by the fact that the introduction of the endoscope guiding tube into the sand during the realization of the test creates a path of preferential drainage. Indeed, in this way, a portion of the intergranular air bubbles close to the surface are able to go up to the surface more easily than those located in-depth. Bubbles present in-depth tend to amalgamate to form macro bubbles.

The important variations noticed during the major parts of the survey probably come from the mode of deposit of the sand (set up coarsely by "package") where air was trapped in a heterogeneous way, leading to the creation of macro pores and thus to very different sized bubbles.

The surfacic air content ratio was weaker in tests 3 and 4 (performed in the denser sand and set up by pluviation). Moreover, a light decrease (from 4% to 3%) can be noticed in-depth due to an increase in the sand density at the bottom of the tank. The size of the bubbles is definitely lower than for surveys 1 and 2. This can be explained by the preparation mode and the density state of the sand. The number of bubbles per image remains relatively constant.

These results confirm the observations of Benhamed et al. (2004) on the importance of the initial structure of sand in the liquefaction phenomenon.

The technical feasibility and the scientific interest in geoendoscopy on underwater soils have been validated by the laboratory tests. It seems that qualitative and quantitative information can be obtained with this method, which is why the next step (consisting of testing the technique in a real situation) was launched.

The laboratory tests highlighted the problem related to equipment implementation in the soil. As a matter of fact, the introduction of the geoendoscopic probe probably caused modifications to the soil structure. This is the reason why, during the in situ experiment, a tube was placed in the soil and measurements were realized only after the completion of an entire tide eventwith the tube in place.

On site air content measurements

The tests carried out in real conditions have highlighted several phenomena. First of all, the device was able to (*i*) measure the evolution of the level of the sand bed during a tide, (*ii*) evaluate the influence of the passage of a wave on the changes of the ground, and (*iii*) visualize the phenomenon of deposit of the grains during the passage of the swell.

It was observed that a great quantity of sediment can be moved during the tide (Fig. 5). Indeed, during our experiment, measurements on other tides using other tools (Cassen et al. 2004; Mory et al. 2004, 2007) evaluated heights of sand bed variation going up to 2 m. For these moved sediments, there is no doubt that any trapped air is evacuated at the time of the transport by the swell. However, for the subbases it has been observed that air remained imprisoned throughout the tide (Fig. 11*a*).

Indeed, the observation with the geoendoscope of the higher fringe of ground during the passage of a single wave highlighted the weak influence of a wave on the basement. It seems that only a few centimetres of sand were moved during the passage of a wave. Thus, in spite of the increase of the tide and the increase of the water table in the soil layers, air can remain trapped. The images and the results obtained at the end of the rising tide (Fig. 11*a*, 12) prove this reasonably well.

The results presented in Fig. 12 were obtained as a result of the geoendoscope being in a still position during an entire tide. From regularly acquired images (approximately each half hour), we could assess after image processing (Fig. 11) the evolution of the quantity of air trapped in the ground during the tide. Figure 12 provides the distribution of the surface air content ratio within the soil according to the depth for two distinct moments of the tide (14:45 and 16:30 end of tide).

The major result of the geoendoscopic tests is the proven existence of a significant presence of air deep inside the soil (Fig. 11*a* and 12), that is, down to 60 cm in the investigated case. This air presence is important, more especially because these results were obtained at the end of the rising tide, whereas the level of water above the ground-level was 1 to 2 m and the sea had reached this level for more than 2 h.

Air content is not constant according to the depth. A thin layer (about 10 cm) of saturated soil is observed in the upper part of the sea bed. Below this layer, down to about 60 cm, air is confined and remains so during the entire tide period, even though a few air bubbles can be seen going up to the surface. In this sand layer, which is not altered by the tide, air content tends to decrease according to the depth. This can be seen on the air content evolution between 14:45

Fig. 12. Surface air content ratio versus depth (during a tide).

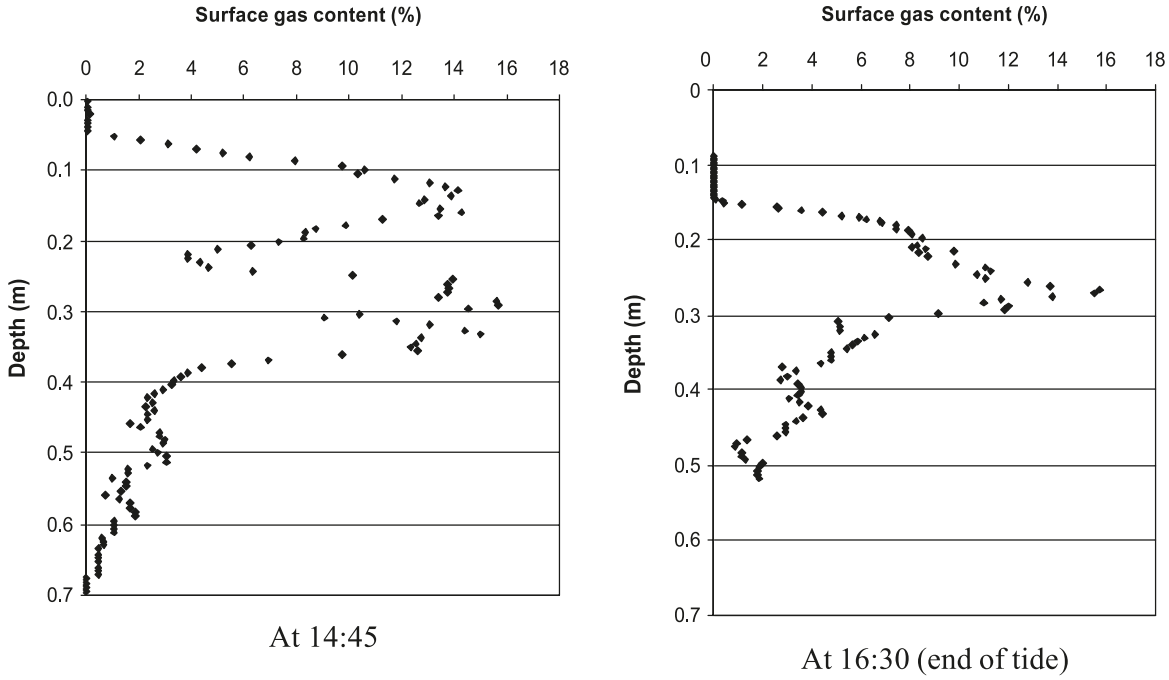

Fig. 13. Relationship between the surfacic air content A_{Ag} and the volumetric air content V_{Vg}.

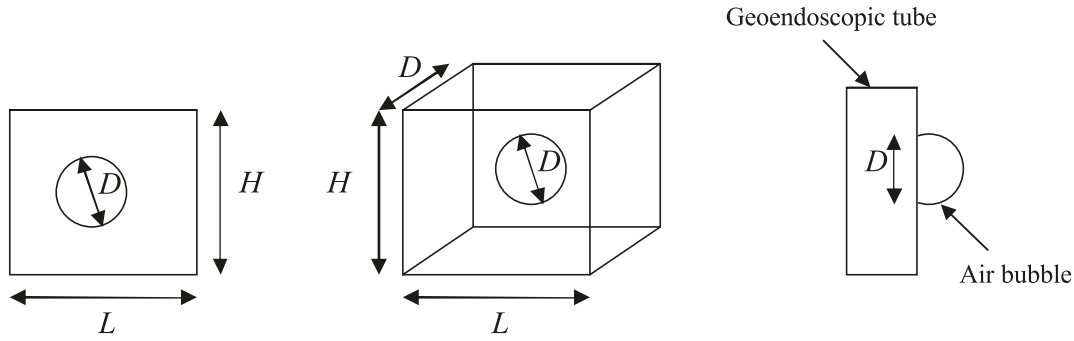

Geoendoscopic image	Volumetric air content	Due to the geoendoscopic tube presence
Image surface $S = LH$	Volume $V = SD$	Air surface $A_g = \pi D^2/4$
Air surface $A_g = \pi D^2/4$	Air Volume $V_g = \pi D^3/6$	Air Volume $V_g' = 0.5\ V_g$
Surfacic air content $A_{A_g} = A_g/S$	Volumetric air content $V_{V_g} = V_g/V$	$V_{V_g} = V_g'/V$

and 16:30. This evolution is due to the increase of the water table pushing the air upwards. Below this layer of unsaturated soil, which corresponds to the layer of sand drained at low tide, saturated soil is again observed. The thickness of the saturated layer observed in the upper part of the sand layer is obviously linked to the strength of the tide and to the amount of sand displaced by the waves that provokes the upward escape of bubbles.

At 16:30, about 10 cm of sediment was removed and consequently the sand was completely saturated until 15 cm.

The "surfacic air content", denoted A_{Ag}, was determined from image analysis. It is defined as the area of the air bubbles in an image divided by the total area of the image. The surfacic air content values can range up to 16%. Volumetric air content evaluation is not trivial to obtain.

In a first approximation, a relationship between the surfacic air content A_{Ag} and the volumetric air content V_{Vg}, defined as the volume of air inside a volume of soil, can be established, assuming that bubbles are spherical and that the depth of focus is the bubble diameter (D) (Fig. 13):

$$[1] \qquad V_{V_g} = 2A_{A_g}/3$$

This relation does not take into account the edge effects due to the presence of the geoendoscopic tube. Moreover, it

also neglects the fact that the air bubbles observed tend to stick and flatten against the Plexiglas geoendoscopic tube. Given these assumptions, the air bubbles observed on the image have a diameter D and a volume V equivalent to a half sphere of diameter D (Fig. 13).

Without the geoendoscopic tube, the air bubbles would have the same volume V but a lower diameter than what was observed because the spheres would be complete.

Given these assumptions, the relationship between the surfacic air content A_{Ag} and the volumetric air content V_{Vg} becomes:

$$[2] \qquad V_{V_g} = A_{A_g}/3$$

Proper calibration is still needed to accurately determine correlations between this surface air content ratio and the volumetric one. This would then enable a saturation degree to be calculated.

Conclusions and perspectives

The focus of the field experiments carried out at Capbreton was to observe the occurrence of liquefaction in the vicinity of a coastal structure subject to wave forcing and also to study the technical feasibility and the reliability of the geoendoscopic technique for determining on site characterization of underwater soil.

This technique demonstrated its suitability for in situ characterization of underwater soils. Soil stratigraphy, grain size distribution, and sea bed evolution have been characterized by this device. Moreover, this methodology clearly showed the existence of a significant air content trapped within the soil during a tide period. An assessment of this content and its evolution during a tide has been measured.

To our knowledge, this is the first time this phenomenon has been observed in situ. These data will be important to thoroughly study the local liquefaction phenomena on coastal structures.

Sakai's model (Sakai et al. 1992) suggested that air content can reach up to a few percents in the sediment layer. The tests carried out with geoendoscopy seem to confirm this order of magnitude of air content. This indicates the very promising features of geoendoscopy for studying liquefaction and, more generally, water flow and soil interactions.

Nevertheless, this important conclusion from our field experiment should be handled with care and not be stated as a general conclusion. The sea was fairly calm in the course of the final field trial during which geoendoscopy was employed, and the presence of air inside the soil was clearly caused by the tidal variations. Some of our video measurements inside the soil have clearly shown that the mobility of soil grains helps air bubbles to escape from the soil. Thus, during an active tide period, the assumption that a great quantity of sediment is moved seems realistic and that explains why the ground becomes completely saturated. The presence of air inside the soil in rougher wave conditions will be discussed more extensively in relation to the measurements made by Sandven et al. (2007) at Capbreton.

Finally, the air content ratio measured is a surfacic content; an accurate correlation with the volumic air content and with the calculation of the degree of saturation remains to be determined. Complementary tests of calibration and parameter setting will undoubtedly be necessary in the next study.

References

Bacconnet, C., Boissier, D., Gourvès, R., and Lepetit, L. 2005. Diagnosis method for liquefaction risk analysis. *In* Fiabilité des matériaux et des structures 4éme conférence nationale « JNF'05 », LGC, Université Blaise Pascal, France, Clermont-Ferrand, 25–26 October 2005. pp.1–10.

Benhamed, N., Canou, J., and Dupla, J.-C. 2004. Structure initiale et propriétés de liquéfaction statique d'un sable. Comptes Rendus de l'Académie des Sciences (Mécanique), **332**(11): 887–894.

Bonjean, D., Foray, P., Piedra-Cueva, I., Michallet, H., Breul, P., Haddani, Y., Mory, M., and Abadie, S. 2004. Monitoring of the foundations of a coastal structure submitted to breaking waves: occurrence of momentary liquefaction. *In* Proceedings of the 14th International Offshore and Polar Engineering Conference and Exhibition, ISOPE 2004, Toulon, France, 23–28 May 2004. Vol. 2. pp. 585–593.

Breul, P. 1999. Caractérisation endoscopique des milieux granulaires couplée à l'essai de pénétration. Thèse de docteur, ingénieur de l'Université Blaise Pascal, Clermont-Ferrand. p. 280.

Breul, P., and Gourves, R. 2003. Rapports d'essais: Liquéfaction des sables en littoral. Synthèse des essais réalisés au laboratoire 3S de Grenoble le 28 janvier 2003. Rapport d'essai n°1 et 2 – LERMES Université Blaise Pascal, Clermont-Ferrand. p. 30.

Breul, P., Gourves, R., and Boissier, D. 1999. Granular materials characterisation by using endoscopy. *In* Proceedings of the International Symposium on Imaging Applications in Geology: Geovision '99, Liège, 6–7 May 1999. pp. 29–32.

Cassen, M., Abadie, S., Arnaud, G., and Morichon, D. 2004. A method based on electrical resistivity measurements to monitor local depth changes in the surf zone and in depth soil response to the wave action. *In* Proceedings of the 29th ICCE International Conference on Coastal Engineering, Lisbon, Portugal, 19–24 September 2004. Vol. 3. pp. 2302–2313.

Chaigneau, L. 2001. Caractérisation des milieux granulaires de surface à l'aide d'un pénétromètre. Thèse de doctorat, Université Blaise Pascal, Clermont-Ferrand. p. 204.

Glaser, S.D., and Chung, R.M. 1998. Estimation of liquefaction potential by in situ methods. Earthquake Spectra, **11**(3): 431–455. doi:10.1193/1.1585822.

Gourvès, R. 1991. Le PANDA – pénétromètre dynamique léger à énergie variable. LERMES CUST, Université Blaise Pascal, Clermont-Ferrand 1991. 12 p.

Gratiot, N., and Mory, M. 2000. Wave induced sea bed liquefaction with application to mine burial. *In* Proceedings of the 10th ISOPE International Offshore and Polar Engineering Conference. Seattle, Wash., 28 May – 2 June 2000. Vol. 2. pp. 600–605.

Grozic, J.L., Robertson, P.K., and Morgenstern, N.R. 1999. The behavior of loose gassy sand. Canadian Geotechnical Journal, **36**(3): 482–492. doi:10.1139/cgj-36-3-482.

Grozic, J.L.H., Robertson, P.K., and Morgenstern, N.R. 2000. Cyclic liquefaction of loose gassy sand. Canadian Geotechnical Journal, **37**(4): 843–856. doi:10.1139/cgj-37-4-843.

Grozic, J.L.H., Imam, S.M.R., Robertson, P.K., and Morgenstern, N.R. 2005. Constitutive modeling of gassy sand behaviour. Canadian Geotechnical Journal, **42**(3): 812–829. doi:10.1139/t05-015.

Haddani, Y. 2004. Classification et caractérisation des milieux

granulaires par géoendoscopie. Thèse de doctorat, Université Blaise Pascal, Clermont-Ferrand. p. 258.

Howa, H., Salomon, J.N., and Tastet, J.P. 1999. Littoral aquitain. Acquis Sciences n°20.

Köhler, H.J., and Koenders, M.A. 2003. Direct visualisation of underwater phenomena in soil–fluid interaction and analysis of the effect of an ambient pressure drop on unsaturated media. Journal of Hydraulic Research, **41**(1): 69–78.

Lepetit, L. 2002. Etude d'une méthode de diagnostic de digues avec prise en compte du risque de liquéfaction, Thèse de doctorat, Université Blaise Pascal. p. 207.

Lepetit, L., Bacconnet, C., Boissier, D., and Gourvès, R. 2002. Etude d'une méthode de diagnostic des digues. Annales du Bâtiment et des Travaux Publics, **2**: 67–73.

Mei, C.C., and Foda, M.A. 1981. Wave induced responses in a fluid-filled poroelastic solid with a free surface – a boundary layer theory. Geophysical Journal of the Royal Astronomical Society, **66**: 597–631.

Mory, M., Michallet, H., Abadie, S., Piedra-Cueva, I., Bonjean, D., Breul, P., and Cassen, M. 2004. Observations of momentary liquefaction caused by breaking waves around a coastal structure. *In* Proceedings of the 29th ICCE International Conference on Coastal Engineering, Lisbon, Portugal, 19–24 September 2004. Vol. 3.

Mory, M., Michallet, H., Bonjean, D., Piedra-Cueva, I., Barnoud, J.M., Foray, P., Abadie, S., and Breul, P. 2007. Field study of momentary liquefaction caused by waves around a coastal structure. Journal of Waterway, Port, Coastal, and Ocean Engineering, **133**(1): 28–38. doi:10.1061/(ASCE)0733-950X(2007)133:1(28).

Rad, N.S., and Lunne, T. 1994. Gas in soil. I: Detection and η-profiling. Journal of Geotechnical Engineering, **120**(4): 697–715. doi:10.1061/(ASCE)0733-9410(1994)120:4(697).

Rad, N.S., Vianna, A.J.D., and Berre, T. 1994. Gas in soils. II: Effect of gas on undrained static and cyclic strength of sand. Journal of Geotechnical Engineering, **120**(4): 716–736. doi:10.1061/(ASCE)0733-9410(1994)120:4(716).

Robertson, P.K., and Wride, C.E. 1998. Evaluating cyclic liquefaction potential using the cone penetration test. Canadian Geotechnical Journal, **35**(3): 442–459. doi:10.1139/cgj-35-3-442.

Sakai, T., Hatanaka, K., and Mase, H. 1992. Wave-induced effective stress in sea bed and its momentary liquefaction. Journal of Waterway, Port, Coastal, and Ocean Engineering, **118**(WW2): 202–206. doi:10.1061/(ASCE)0733-950X(1992)118:2(202).

Sandven, R., Husby, E., Husby, J.E., Jønland, J., Roksvåg, K.O., Stæhli, F., and Tellugen, R. 2007. Development of Sampler for measurement of gas content. Journal of Waterway, Port, Coastal, and Ocean Engineering, **133**(1): 3–13. doi:10.1061/(ASCE)0733-950X(2007)133:1(3).

Seed, H.B., and De Alba, P. 1986. Use of SPT and CPT tests for evaluating the liquefaction resistance of sands. *In* Proceedings of In Situ ?86, a Specialty Conference Sponsored by the Geotechnical Engineering Division of the ASCE. Geotechnical Special Publications, ASCE, Vol. 6, pp 281–302.

Zhou, S. 1997. Caractérisation des sols de surface à l'aide du pénétromètre dynamique léger de type Panda. Thèse de doctorat Université Blaise Pascal. p. 178.